Remote Sensing for Environmental Monitoring and Change Detection (Proceedings of Symposium HS3007 at IUGG2007, Perugia, July 2007). IAHS Publ. 316, 2007.

Assessing crop water deficit using MODIS data during winter wheat growing period along the lower reaches of the Yellow River, China

YONGHONG YI[1], DAWEN YANG[1], HUIMIN LEI[1] & TAIKAN OKI[2]

1 *State Key Laboratory of Hydroscience and Engineering, Department of Hydraulic Engineering, Tsinghua University, Beijing 100084, China*
yiyh05@mails.tsinghua.edu.cn

2 *Institute of Industrial Science, University of Tokyo, Tokyo, Japan*

Abstract The Weishan Irrigation Zone along the lower reaches of the Yellow River consists of a total irrigated area of 3600 ha. The region has an average annual rainfall of 500–600 mm, with 60–70% of local rainfall occurring during the summer, and with less than 15% in spring. The water deficit during the spring affects the winter wheat growth from March to early June, which is a major growth period significantly impacting overall wheat production. Remote sensing has been an efficient guide for irrigation agriculture by providing regional estimates of crop water deficits. Daily Terra and Aqua MODIS surface reflectance and temperature products from March to June 2006 were collected and the Surface Energy Balance System (SEBS) was applied to model the turbulent energy flux. A drought severity index (DSI) derived in SEBS and the normalized difference water index (NDWI) were used to evaluate the canopy water deficit during the growing period. Combing with *in situ* soil moisture and crop growth observations, it was found that DSI can provide reasonable estimates of crop water deficits. NDWI can be used as an index for vegetation water content (VWC) but can not be used for crop water stress detection without knowing the ideal status of crop growth.

Key words DSI; crop water deficit; MODIS; NDWI; SEBS

INTRODUCTION

Water availability is considered a major limiting factor for crop growth in the Northern China Plains (NCP) region, where irrigation has been indispensable in ensuring high crop yields. Monitoring crop water stress in combination with efficient irrigation patterns is helpful in relieving the pressure on scarce local water resources. Irrigation scheduling methods are generally based on measurements of soil water content or meteorological parameters for actual evaporation estimation, which is frequently not accurate and timely for regional crop water stress detection. Satellite-based indicators have the advantage of monitoring real-time spatial and temporal variations in water stress at regional, continental and even global scales, as a result of frequency and the global extent of coverage (Su *et al*., 2003). The Terra and Aqua MODIS instruments provide daily coverage with higher spectral and spatial resolution than was previously possible with SPOT-VEGETATION and AVHRR observations. In this study, we discuss the possibilities of using MODIS data for the detection of crop water deficits during the winter wheat growing season. Two indices, including NDWI and a drought

index derived in SEBS, were evaluated with daily rainfall and *in situ* soil moisture observations.

METHODOLOGY

Surface Energy Balance System

The SEBS model (Su, 2002) was developed for estimating atmospheric turbulent fluxes based on the surface energy balance index (SEBI) concept. According to Menenti & Choudhury (1993), the relative evaporation, Λ_r, is related to the actual, minimum, and maximum difference between surface and air potential temperature at the reference height, and is expressed as:

$$\Lambda_r = \frac{\lambda E}{\lambda E_p} = 1 - SEBI \tag{1}$$

and

$$SEBI = \left(\frac{\theta_0 - \theta_a}{r_e} - \frac{(\theta_0 - \theta_a)_w}{(r_e)_w} \right) \Bigg/ \left(\frac{(\theta_0 - \theta_a)_d}{(r_e)_d} - \frac{(\theta_0 - \theta_a)_w}{(r_e)_w} \right) \tag{2}$$

where λE is the actual latent heat flux density, λE_p is the potential latent heat flux density, θ_0 is the surface potential temperature (K), θ_a is the potential temperature of air at reference height, the subscript w indicates the wet limiting condition with minimum temperature difference and the subscript d indicates the dry limiting condition with maximum temperature difference. The surface–air temperature difference is given as:

$$T_0 - T_a = \frac{\frac{r_i + r_e}{\rho C_p}(R_n - G) - \frac{e^* - e}{\gamma}}{1 + \frac{\Delta}{\gamma} + \frac{r_i}{r_e}} \tag{3}$$

where ρ is the air density (kg m^{-3}), C_P is the specific heat of air at constant pressure (1005 J kg^{-1} K^{-1}), e is actual vapour pressure near surface (Pa), e^* is the saturated vapour pressure (Pa) at mean air temperature, Δ is the slope of e^* at air temperature, γ is the psychrometric constant, r_i is the bulk surface internal resistance (s m^{-1}); r_e is the aerodynamic resistance (s m^{-1}), and is expressed as:

$$r_e = \frac{1}{k u_*} \left[\ln\left(\frac{z-d}{z_{0h}}\right) - \psi_m\left(\frac{z-d}{L}\right) + \psi_h\left(\frac{z_{0h}}{L}\right) \right] \tag{4}$$

where k is von Karman's constant (0.4), u_* (m s^{-1}) is the friction velocity, d (m) is the zero plane displacement height, z_{0k} (m) is the roughness height for heat transfer, Ψ_m and Ψ_h are the stability correction functions for momentum and sensible heat transfer, respectively, and L is the Monin-Obukhov length defined as:

$$L = -\frac{\rho u_*^3}{kg\left(\frac{H}{T_a C_p} + 0.61E\right)} \tag{5}$$

where g is the acceleration due to gravity (m s^{-2}).

In wet conditions, evaporation takes its potential value. This is the case for $r_i \to 0$ in equation (3) and the wet boundary of surface-air temperature difference is therefore:

$$(T_0 - T_a)_w = \frac{\frac{(r_e)_w}{\rho C_p}(R_n - G) - \frac{e^* - e}{\gamma}}{(1 + \frac{\Delta}{\gamma})} \tag{6}$$

In dry conditions evaporation becomes zero due to the limitation of water availability in soil and the sensible heat flux density takes its maximum value. This is corresponding to the case for $r_i \to \infty$ in equation (3) and the dry boundary of surface–air potential temperature difference is:

$$(T_0 - T_a)_d = \frac{(r_e)_d (R_n - G)}{\rho C_p} \tag{7}$$

To estimate sensible heat flux at regional scales, bulk atmospheric boundary layer similarity stability functions should be used to obtain the stability correction functions Ψ_m and Ψ_h. The Broyden method was applied to solve friction velocity, the sensible heat flux, and the Obukhov stability length (Su, 2002).

In SEBS, the surface energy balance is written as:

$$R_n = G_0 + H + \lambda E \tag{8}$$

where R_n is the net radiation. The net radiation flux density is estimated as:

$$R_n = (1 - \alpha) R_{swd} + \varepsilon R_{lwd} - \varepsilon \sigma T_0^4 \tag{9}$$

where α is the albedo, R_{swd} and R_{lwd} are the downward solar radiation and longwave radiation, respectively, ε is the emissivity of the surface, σ is the Stefan-Bolzmann constant, and T_0 is the surface temperature.

The soil heat flux density G is estimated from net radiation:

$$G = R_n \left[\Gamma_c + (\Gamma_s - \Gamma_c) \cdot (1 - f_c) \right] \tag{10}$$

where f_c is the fractional vegetation cover, Γ_s and Γ_c are the ratios of G to R_n for bare soil and fully vegetated surfaces, respectively. Values for Γ_s and Γ_c were taken as 0.315 and 0.05, respectively.

Su *et al*. (2003) developed a drought severity index (*DSI*) directly related to the relative evaporation in order to quantify the soil water deficit in the root zone:

$$DSI = 1 - \frac{H - H_{wet}}{H_{dry} - H_{wet}} = 1 - \Lambda_r \tag{11}$$

Normalized Difference Water Index

NDWI was first proposed by Gao (1996) in a manner similar to *NDVI*, however, with the visible channel by another near infrared (NIR) channel at 1.24 μm, and expressed as:

$$NDWI = \frac{\rho_{NIR} - \rho_{SWIR}}{\rho_{NIR} + \rho_{SWIR}} \tag{12}$$

where ρ_{NIR} and ρ_{SWIR} are the reflectances of the *NIR* and shortwave infrared (*SWIR*) channels, respectively. Carter (1994) pointed out that increased reflectance in *SWIR* wavelengths was the most consistent leaf reflectance response to plant stress in general including water stress. Tucker (1980) concluded that the 1.55–1.75 μm region was the best suited wavelength interval for satellite-platform remote sensing of plant canopy water status. For this study, MODIS band 7 (2.13 μm) was used to define *NDWI*, since band 6 (1.64 μm) of the Aqua MODIS sensor was noisy.

Data description

Field experiments were carried out at the Gaoying station (116°3′15.3″E, 36°38′ 55.5″N, and 30 m elevation) in the Weishan Irrigation Zone (115°24′–116°30′E, 36°12′– 37°00′N) (Fig. 1) during the 2006 growing season of winter wheat. The irrigated zone is the fifth largest irrigation zone in China, and also the largest irrigated zone along the downstream of the Yellow River. The average precipitation in this zone is about 571 mm/year, of which over 60% falls during the summer. Rotation of winter wheat and summer corn is the major crop plantation form. Turbulent energy flux densities were measured automatically from the eddy flux tower with precipitation and two soil moisture profiles at depths of 5, 10, 20, 40, 80 and 160 cm simultaneously from a groundwater network. Crop growth parameters including *LAI*, *VWC* and crop height were measured five times from 1 April to 3 June. Irrigation data, which included discharge and date, have been collected since February 2006.

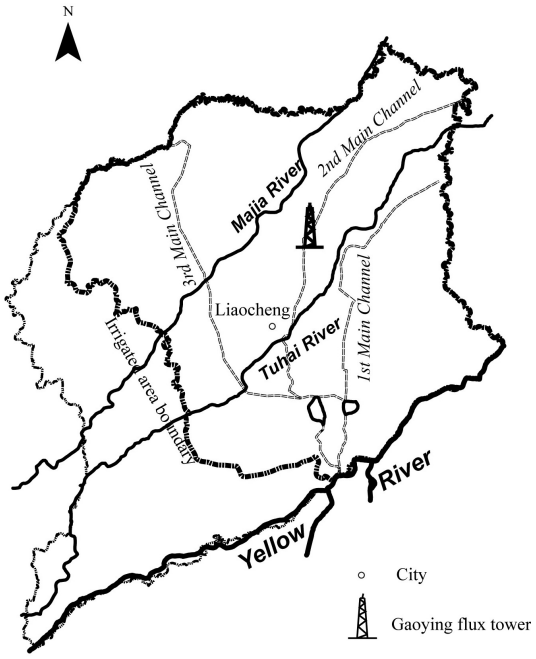

Fig. 1 The Weishan Irrigation Zone along the downstream of the Yellow River and the location of the flux tower.

MODIS 500 m daily surface reflectance and 1 km surface temperature products were used to run the SEBS model and calculate the *NDWI* index. For the *NDWI* calculation, the image was excluded if the cloud and mixed area in the study region exceeded 30% or the blue band reflectance was above 0.07 to eliminate undetected cloud effects. About 15 Terra and 13 Aqua MODIS data sets were eventually selected for the analysis.

RESULTS AND DISCUSSION

Validation of SEBS

The outputs of SEBS were compared with the two measured energy balance terms, which consisted of a 30-min average around the local overpass time of Terra and Aqua satellites (see Fig. 2). The estimated and measured sensible heat flux agreed well with a mean bias of about 25 W m^{-2}, while the estimated latent heat flux was mostly larger than the measured, especially for Terra MODIS. The R^2 values between the estimated and observed latent heat flux were 0.87 for Terra MODIS, and 0.70 for Aqua MODIS. The regressions for the two relationships were computed as:

$$LE_{sebs} = 1.1007 LE_{obv} + 56.022 \quad (13)$$

and

$$LE_{sebs} = 1.0009 LE_{obv} + 48.216 \quad (14)$$

respectively. Flux observations demonstrated that the energy imbalance was quite large on some days, with a close relation to the bias between the observed and modelled turbulent latent heat flux. This could result from the underestimation of turbulent heat fluxes at the flux tower, which occurred at some sites according to the FLUXNET (Baldocchi *et al*., 2001). However, the remaining terms in the energy balance equation were omitted in the SEBS model, including the advection energy, energy stored in the canopy layer etc., which could also contribute to the error in the estimate of instantaneous fluxes. Additionally, we can also expect some differences between the 30-minute averaged flux observations and the instantaneous SEBS model output.

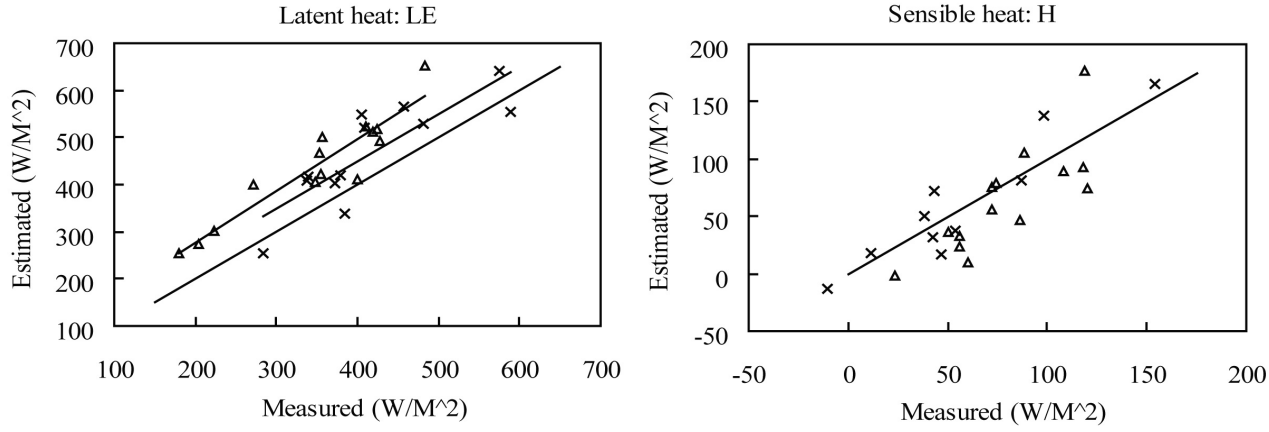

Fig. 2 SEBS estimated *vs* measured latent and sensible heat fluxes, with triangle for Terra MODIS and cross for Aqua MODIS.

Evaluating crop water stress using DSI and NDWI

The response of DSI and NDWI to the soil moisture changes during the wheat growing period was analysed together with daily rainfall and averaged volumetric root zone soil moisture (0–40 cm) (Fig. 3).

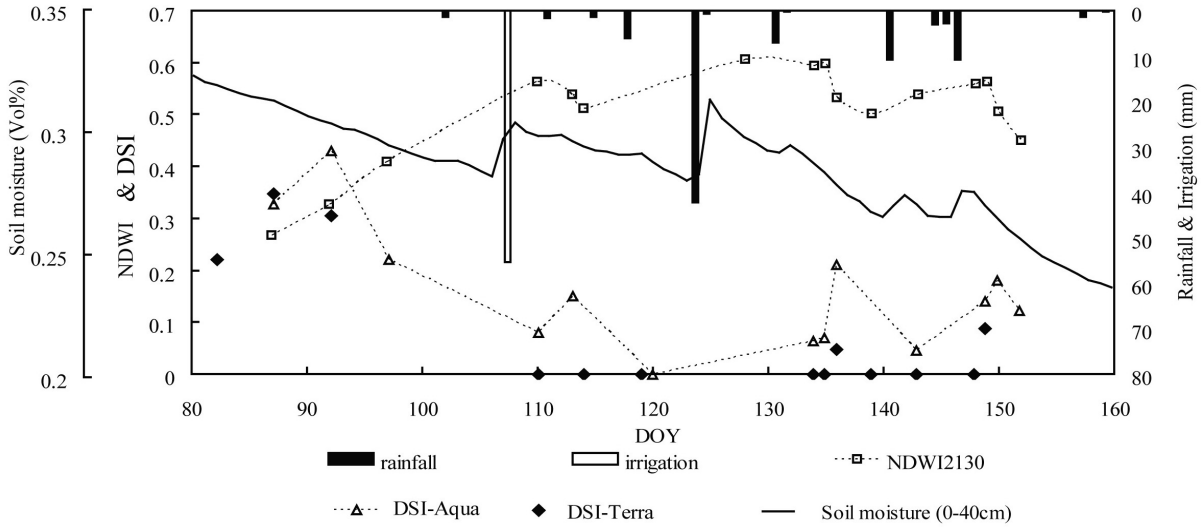

Fig. 3 Response of *NDWI* and *DSI* to soil moisture changes from March to June, 2006. *In situ* rainfall and averaged soil moisture at 0–40 cm depth, $NDWI_{2130}$, DSI-Aqua and DSI-Terra were combined into analysis.

DSI-Aqua was found to be larger than DSI-Terra especially during the later part of the growing, although the different overpass times of the two satellites may have contributed to these differences. Local overpass time for Terra and Aqua were around 10:30 and 13:30 h, respectively. Much research has observed diurnal changes in the crop water deficit, peaking around 14:00 h, which is usually just after the solar noon and which may be closely related to other phenomena that occurs around this time, for instance peaks in radiation, air temperature, crop stomatal resistance, etc. (Sepulcre-Canto *et al*., 2006). Both Terra and Aqua DSI indicated that wheat experienced severe water deficit before DOY 97, while the root zone soil moisture remained relatively high. However, field observations at DOY 91 showed that the wheat root biomass was concentrated mostly within a 0–5 cm surface layer. Soil moisture values at 5 cm were found to be only 0.296 at DOY 80 to 0.262 at DOY 110, and below 0.2 after DOY 110. Under normal growing conditions with adequate soil moisture, wheat crop roots will typically penetrate well into 0–40 cm zone. However, as observed in this study, this is not the case under drier growing conditions.

Figure 4(b) shows the temporal changes in *VWC* and *NDWI* during the winter wheat growth period. It can be seen that *NDWI* can be used as an index of vegetation water content. From Fig. 4, we can see that *NDWI* continues to increase until DOY 110, due to the rapid crop growth with LAI increasing nearly from 1 to 6, even when soil moisture continued to decrease (see Fig. 3). After a brief decline around DOY 110, NDWI continued to increase and peak around DOY 128 due to increased rainfall.

After DOY 110, *NDWI* was found to be strongly affected by the rainfall and the changes in soil moisture. From DOY 110 to 159, the R^2 value between *NDWI* and soil moisture at 0–10 cm was 0.80, while only 0.44 for soil moisture at 0–160 cm.

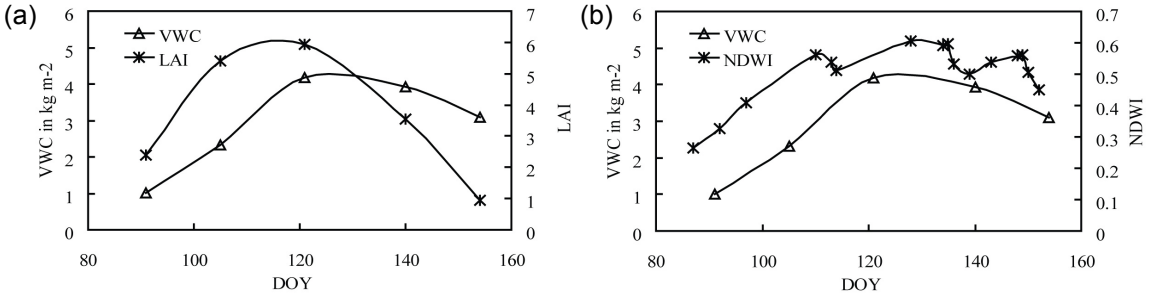

Fig. 4 (a) The temporal variations of measured *LAI* and *VWC* during wheat growing period. (b) The temporal variations of *NDWI* and measured *VWC*.

The temporal changes in soil moisture and measured crop parameters were used to evaluate the crop water deficiency. The volumetric soil moisture at field capacity was about 0.37, calculated using the Van Genuchten equation with field calibrated parameters. Usually, the soil water content in the root zone should be about 75–80% of field capacity for optimum wheat growth during the retrieval stage and a little lower after grain filling. Before the jointing stage (around DOY 97), the top soil layer was unable to satisfy the crop water demand, which was reflected by a relatively high DSI value. However, it is difficult to determine from the *NDWI* alone whether the wheat was under water stress because *NDWI* continued to increase due to the increasing *VWC* in the crop (See Fig. 4(b)). After DOY 110, there occurred only short-term dry periods between the rainfall events, which are reflected in time series of DSI and NDWI. NDWI was observed to decrease with increasing *VWC* from DOY 110 to 123 and NDWI had a sharp decrease around DOY 136, which implied that the crop experienced water shortage to some extent. The sudden drop of *NDWI* after DOY 149, kept the same trend as the soil moisture and *VWC* changes in the maturing stage. These trends appeared to have little to do with water shortage. Comparatively, the water deficit during the later period was much less than during the early period. The R^2 between the Aqua DSI and *NDWI* was calculated as 0.74. However, as discussed above, DSI can provide an indication crop water deficiency while *NDWI* is helpful only when the ideal crop growing conditions are known.

CONCLUSIONS

NDWI and a drought index (DSI) derived from SEBS model were used to evaluate the crop water deficiency during the winter wheat growing season. DSI was found to provide a reasonable indication of the crop water deficit based on an analysis of the soil moisture changes and the crop growth status. The result showed that the wheat encountered relative greater water stress prior to the jointing stage (DOY 97) when most of the root biomass was concentrated within the 0–5 cm surface layer, and the

soil moisture within this zone was unable to satisfy the wheat water demand at the retrieval period. After the jointing stage, the wheat can utilize the soil water at the deeper layer together with the irrigation at DOY 107 and increasing rainfall, all of which contributed to relieving the crop water stress. After that, only short-term water deficits were experienced between rainfall events with DSI basically less than 0.2. The temporal changes of *NDWI* and DSI were found highly correlated (R^2 = 0.74). However, *NDWI* was found to be closely related with the soil moisture changes only during the later growth period (after DOY 110). Therefore, *NDWI* can be considered a poor indicator of crop water stress without knowledge of optimum crop growth characteristics.

Acknowledgements This research was partially supported by the National Natural Science Foundation of China (50679029) and by the National 973 Project of China (2006CB403405). Thanks were given to Dr. Su (ITC, Netherlands) to provide the SEBS code for evaporation modelling.

REFERENCES

Baldocchi, D., Falge, E., Gu, L. *et al*. (2001) FLUXNET: a new tool to study the temporal and spatial variability of ecosystem-scale carbon dioxide, water vapor, and energy flux densities. *Bull. Am. Met. Soc.* **82**, 2415–2434.

Carter, G. A. (1994) Ratios of leaf reflectances in narrow wavebands as indicators of plant stress. *Int. J. Remote Sens.* **15**, 697–703.

Gao, B. (1996) *NDWI*—a normalized difference water index for remote sensing of vegetation liquid water from space. *Remote Sens. Environ*. **58**, 257–266.

Menenti, M. & Choudhury, B. J. (1993) Parameterization of land surface evapotranspiration using a location-dependent potential evapotranspiration and surface temperature range. In: *Exchange Processes at the Land Surface for a Range of Space and Time Scales* (ed. by H. J. Bolle, R. A. Feddes & J. D. Kalma), 561–568. IAHS Publ. 212. IAHS Press, Wallingford, UK.

Sepulcre-Canto, G., Zarco-Tejada, P. J., Jimenez-Munoz, J. C., Sobrino, J. A., Miguel, E. & Villalobos, F. J. (2006) Detection of water stress in an olive orchard with thermal remote sensing imagery. *Agric. For. Met.* **136**, 31–44.

Su, Z. (2002) The surface energy balance system (SEBS) for estimation of turbulent heat fluxes. *Hydrol. Earth System Sci.* **6**(1), 85–89.

Su, Z., Yacob, A., Wen, J., Roerink, G., He, Y., Gao, B., Boogaard, H. & Diepen, C. (2003) Assessing relative soil moisture with remote sensing data: theory, experimental validation, and application to drought monitoring over the North China Plain. *Phys. Chem. Earth* **28**, 89–101.

Tucker, C. J. (1980) Remote sensing of leaf water content in the near infrared. *Remote Sens. Environ.* **10**, 23–32.